(2)

HDL-TM-90-20

December 1990

Host Materials for $4d^N$ and $5d^N$ Transition-Metal Ions

by Clyde A. Morrison

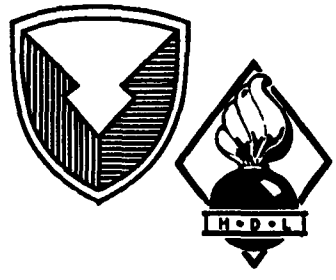

U.S. Army Laboratory Command
Harry Diamond Laboratories
Adelphi, MD 20783-1197

The findings in this report are not to be construed as an official Department of the Army position unless so designated by other authorized documents.

Citation of manufacturer's or trade names does not constitute an official endorsement or approval of the use thereof.

Destroy this report when it is no longer needed. Do not return it to the originator.

REPORT DOCUMENTATION PAGE

Form Approved
OMB No. 0704-0188

1. AGENCY USE ONLY *(Leave blank)*	2. REPORT DATE	3. REPORT TYPE AND DATES COVERED
	December 1990	Final

4. TITLE AND SUBTITLE
Host Materials for $4d^N$ and $5d^N$ Transition-Metal Ions

5. FUNDING NUMBERS
PE: 611102.H440011

6. AUTHOR(S)
Clyde A. Morrison

7. PERFORMING ORGANIZATION NAME(S) AND ADDRESS(ES)
Harry Diamond Laboratories
2800 Powder Mill Road
Adelphi, MD 20783-1197

8. PERFORMING ORGANIZATION REPORT NUMBER
HDL-TM-90-20

9. SPONSORING/MONITORING AGENCY NAME(S) AND ADDRESS(ES)
U.S. Army Laboratory Command
2800 Powder Mill Road
Adelphi, MD 20783-1145

10. SPONSORING/MONITORING AGENCY REPORT NUMBER

11. SUPPLEMENTARY NOTES
AMS code: 611102.H440011
HDL PR: AE1051

12a. DISTRIBUTION/AVAILABILITY STATEMENT
Approved for public release; distribution unlimited.

12b. DISTRIBUTION CODE

13. ABSTRACT *(Maximum 200 words)*

This report discusses ten compounds which are potential host materials for quadruply ionized elements with $4d^N$ and $5d^N$ electronic configurations. These compounds are $ZrSiO_4$, $HfGeO_4$, Li_2ZrTeO_6, Li_2HfTeO_6, Li_6BeZrF_{12}, $ZrGeO_4$, $ZrGeO_8$, $ThSiO_4$, and $ThGeO_4$ (in two forms: zircon and scheelite). The crystal-field components, A_{nm}, are calculated for the Zr, Hf, and Th sites in each of the compounds. The site symmetry is S_4 or D_{2d}, except for Li_2XTeO_6 (X = Zr, Hf) which has C_3 symmetry. Approximate parameters, $F^{(k)}$, B_{nm} (B, C, Dq), are given for the entire quadruply ionized $5d^N$ configuration. Energy levels of W^{4+} ($5d^2$) and Re^{4+} ($5d^3$) are given for some compounds.

14. SUBJECT TERMS
Transition metal ions, $5d^N$ electronic configuration, $4d^N$ electronic configuration, tunable laser material

15. NUMBER OF PAGES
49

16. PRICE CODE

17. SECURITY CLASSIFICATION OF REPORT	18. SECURITY CLASSIFICATION OF THIS PAGE	19. SECURITY CLASSIFICATION OF ABSTRACT	20. LIMITATION OF ABSTRACT
Unclassified	Unclassified	Unclassified	UL

Contents

Page

1. Introduction 5

2. Crystallographic Data and Crystal-Field Components 6

3. Hamiltonians for d^N Electronic Configuration in a Crystal 6

   3.1 Free-Ion Hamiltonian 6
   3.2 Crystal-Field 8

4. Cubic Approximation for Each Host 11

   4.1 $ZrSiO_4$ 11
   4.2 $HfGeO_4$ 12
   4.3 Li_2XTeO_6 (X = Zr, Hf) 12
   4.4 Li_6BeZrF_{12} 13
   4.5 $ZrGeO_2$ 14
   4.6 Zr_3GeO_8 14
   4.7 $ThSiO_4$ 15
   4.8 $ThGeO_4$ 15

5. Conclusion 16

References 24

Appendix A 25

Distribution 45

Tables

1. Approximate free-ion parameters (cm^{-1}) and values of ρ_n ($Å^n$) for the quadruply ionized ions with the $5d^N$ configuration 17

2a. Energy levels of W^{4+} in the Zr site of $ZrSiO_4$, cubic approximation 18
2b. Energy levels of W^{4+} in the Zr site in $ZrSiO_4$ 19
2c. Energy levels of Re^{4+} in the Zr site in $ZrSiO_4$, cubic approximation 20
2d. Energy levels of Re^{4+} in the Zr site of $ZrSiO_4$ 21

3a. Energy levels of W^{4+} in the Zr site in Li_2ZrTeO_6, cubic approximation 22
3b. Energy levels of W^{4+} in the Zr site in Li_2ZrTeO_6 23

1. Introduction

The spectra of the $4d^N$ and $5d^N$ electronic configurations are very limited, both in the solid state and the free ion. This is unfortunate since these ions have a number of levels in the infrared and visible spectral regions; because of the various ionization possibilities of each ion, they offer a rich area for possible tunable laser sources.

We wish to investigate the spectra of the $4d^N$ and $5d^N$ quadruply ionized ions in transparent oxide host crystals. This report provides the information we have found concerning these ions and presents a number of host materials which we consider candidates for immediate study.

The situation concerning the $4d^N$ and $5d^N$ transition-metal ions before 1962 is summarized by Ballhausen (1962). More recently, several of the $4d^N$ and $5d^N$ ions have been reported in fluoride or chloride host materials (Morrison, 1989). In this latter reference, six host materials are given for which experimental data have been reported on $4d^N$ and $5d^N$ ions. Unfortunately, in all these hosts, the electric dipole transitions are forbidden by the symmetry of the site occupied by the $4d^N$ or $5d^N$ ion. Consequently, the weak magnetic dipole transitions must be sorted out from relatively strong vibronic transitions. Although this procedure can be done, it directs time and effort away from understanding the crystal-field splitting and developing a model for these splittings. Thus, time would be better spent selecting a host material that does have electric dipole transitions allowed for the site occupied by the $4d^N$ or $5d^N$ ions.

We have selected several host materials in which Hf^{4+}, Zr^{4+}, or Th^{4+} is a constituent that can be replaced substitutionally by a quadruply ionized $4d^N$ or $5d^N$ ion; also, the site occupied by these ions allows electric dipole transitions. In addition, we have selected hosts with the site symmetry high enough for us to analyze (C_3, C_4, and higher) with our present programs. A number of these materials have either Si^{4+} or Ge^{4+} as constituents, and crystal-field components have been calculated for these sites. These sites can be occupied by quadruply ionized $3d^N$ ions, and experimental data have been reported on V^{4+} in several zircon-type crystals considered here (Di Gregario et al, 1982).

Unfortunately, for the hosts we have chosen, the available data are only x-ray data and some crystal growth data, with no experimental data on $4d^N$ and $5d^N$ optical spectra. The $4d^N$ and $5d^N$ transition elements have not been tried as potential lasers possibly because so little experimental data have been taken and their spectra have not been identified. That is, for these ions, we have no method of simply analyzing the experimental data, such as the Tanabe-Sugano diagrams,

which have been so successful for the analysis of the $3d^N$ series spectra. We now have available Tanabe-Sugano-like diagrams for the $4d^N$ and $5d^N$ electronic configurations, which include the large spin-orbit coupling necessary in the analysis of the spectra of these ions. We intend to publish these diagrams in the near future, including the diagrams of quadruply ionized $5d^N$ ions for tetrahedral symmetry ($Dq/B < 0$), which can be used with the cubic approximation given in this report to predict the spectra of these ions in the host materials considered here.

2. Crystallographic Data and Crystal-Field Components

The tables in the appendix contain the crystallographic and x-ray data on each host. The arrangement of the tables is the same as in Morrison (1989); a detailed discussion of the arrangement is given on page 24 of that reference. These data are used to compute the crystal-field components for a particular site and reflect the symmetry of the site. In the discussion here we use only the monopole crystal-field components; the other contributions to the crystal field are included in anticipation of future possible refinements in the analysis. The crystal-field parameters are given by

$$B_{nm} = \rho_n A_{nm} \ , \tag{1}$$

where the ρ_n are "effective" values of $\langle r^n \rangle$ for a particular ion in the solid. The A_{nm} are given in the tables by Morrison (1989). Since we have no experimental data on these ions in the hosts considered here, we defer the derivation of approximate values of ρ_n until later. The tables on each host are followed by the references to the data given on that host, so that in a certain sense each host material is a complete and separable item.

3. Hamiltonians for d^N Electronic Configuration in a Crystal

3.1 Free-Ion Hamiltonian

The free-ion Hamiltonian for a configuration of d^N electrons is taken as

$$H_{FI} = F^{(2)} g_2 + F^{(4)} g_4 + \zeta \sum_{i=1}^{N} \vec{l}_i \cdot \vec{s}_i \ , \tag{2}$$

with

$$g_k = \sum_{i>j} \sum_{q=-k}^{k} C^*_{kq}(i)\, C_{kq}(j) \,, \tag{3}$$

$$C_{kq} = \sqrt{4\pi/(2k+1)}\, Y_{kq} \,. \tag{4}$$

The $F^{(k)}$ and ζ have been calculated by using Hartree-Fock wavefunctions (Morrison, 1989), and the matrix elements of g_k are given by Neilson and Koster (1963). Frequently the Racah parameters B and C are used in place of the Slater parameters, $F^{(k)}$; the relations (Morrison, 1989, p 29)

$$\begin{aligned} F^{(2)} &= 7(7B + C) \,, \\ F^{(4)} &= (63/5)\, C \,, \end{aligned} \tag{5}$$

can be used to convert from one set of parameters to the other.

In general, the Slater parameters are considerably reduced when the ion enters a solid. Furthermore, these same parameters obtained by fitting the free-ion spectra are less than the corresponding values computed with Hartree-Fock wavefunctions. For example, for Cr^{3+} we obtained the following values (Morrison, 1989, pp 21, 14, and 119):

Parameter	Hartree-Fock calculation	Free-ion experiment	Al_2O_3 experiment
$F^{(2)}$	88,514	74,201	53,690
$F^{(4)}$	55,558	45,822	39,312
B	1,177	994.7	650
C	4,409	3,637	3,120

We see that B decreases from the Hartree-Fock value to the value obtained for Cr^{3+} in Al_2O_3. Further, Dq for Cr^{3+} is 1596 cm^{-1}, so that Dq/B = 2.56. On the other hand, we can compute the Dq using $\langle r^4 \rangle$ from Hartree-Fock values and the crystal-field component, A_{40}. Using equation (1), we obtain Dq = 439.9 cm^{-1} and Dq/B = 0.374, which is considerably less than the value of Dq/B = 2.56 observed in experiment. Dq/B is one of the fundamental quantities extracted from experimental data using a standard Tanabe-Sugano plot. We find that the Hartree-Fock method greatly underestimates the values of Dq/B, compared to experimental data. This is not surprising, since the value of B decreases significantly when an ion enters the solid, whereas the radial wavefunction of the transition-metal ion expands, causing an increase

of $\langle r^4 \rangle$. These two effects cause the ratio Dq/B to increase dramatically.

3.2 Crystal-Field

The crystal-field Hamiltonian appropriate for S_4 and D_{2d} symmetry for the electronic configuration d^N can be written as

$$H_{CEF} = B_{20} \sum_{i=1}^{N} C_{20}(i) + B_{40} \sum_{i=1}^{N} C_{40}(i) + B_{44} \sum_{i=1}^{N} \left[C_{44}(i) + C_{4-4}(i) \right], \qquad (6)$$

with the crystal-field parameters B_{nm} real (Morrison, 1989). Actually the crystal-field Hamiltonian given in equation (6) is valid for the electronic configuration d^N for site symmetries as low as C_4 with B_{nm} real. If the site occupied by the ion has cubic symmetry, then $B_{20} = 0$, $B_{44} = (5/14)^{1/2} B_{40}$, and equation (6) becomes

$$H_{CEF}^{C} = B_{40}^{C} \sum_{i=1}^{N} \left\{ C_{40}(i) + \sqrt{\frac{5}{14}} \left[C_{44}(i) + C_{4-4}(i) \right] \right\}. \qquad (7)$$

In equation (7) if $B_{40} > 0$, then we have octahedral symmetry, and if $B_{40} < 0$, we have tetrahedral symmetry. In both cases, the crystal-field parameter B_{40} is related to Dq by

$$B_{40}^{C} = 21\, Dq \ . \qquad (8)$$

Here, the experimentally determined Dq is often taken positive, and the sign of B_{40} in equation (8) is determined by additional knowledge of the symmetry of the particular site. In the cases considered here, the sign of B_{40} will be taken to be the same as the monopole crystal-field component, A_{40}.

Frequently, it is convenient to assume that the symmetry of the site occupied by the transition-metal ion is approximately cubic and use the rotational invariant (Leavitt, 1982) given by

$$S_4(B) = \sqrt{B_{40}^2 + 2B_{44}^2} \qquad (9)$$

to obtain a value of the crystal-field parameters, B_{40}^C, as

$$B_{40}^C = \sqrt{\frac{7}{12}}\, S_4(B) \quad . \tag{10}$$

Here we have used the result

$$S_{40}^C(B) = \sqrt{\frac{12}{7}}\, B_{40}^C \ , \tag{11}$$

$$B_{44}^C = \sqrt{\frac{5}{14}}\, B_{40}^C \quad . \tag{12}$$

The sign of B_{40}^C in equation (10) must be determined from additional information on the particular site occupied by the transition-metal ion. If detailed x-ray data are available on a particular host material, the crystal-field components, A_{nm}, can be computed and equation (1) used to obtain

$$B_{40}^C = \sqrt{\frac{7}{12}}\, \rho_4\, S_4(A) \tag{13}$$

from equation (11). The sign of B_{40}^C given in equation (11) is then the same as A_{40}. The cubic approximation is good only as long as B_{20} (or A_{20}) ~ 0 and B_{44} (or A_{44}) ~ $(5/14)^{1/2}\, B_{40}(A_{40})$.

If the site occupied by the transition-metal ion has C_3 symmetry or higher, the crystal-field Hamiltonian is

$$H_{CEF} = B_{20} \sum_{i=1}^{N} C_{40}(i) + B_{40} \sum_{i=1}^{N} C_{40}(i) + B_{43} \sum_{i=1}^{N} \left[C_{43}(i) - C_{4-3}(i) \right] \ , \tag{14}$$

where, as before, all B_{nm} are real.

The cubic approximation in this symmetry is given by

$$\begin{aligned} B_{20} &= 0 \ , \\ B_{40}^C &= \sqrt{\frac{10}{7}} B_{40} \ , \end{aligned} \tag{15}$$

and

$$H_{CEF}^{C} = B_{40}^{C} \sum_{i=1}^{N} \left\{ C_{40}(i) + \sqrt{\frac{10}{7}} \left[C_{43}(i) - C_{4-3}(i) \right] \right\} . \tag{16}$$

Also in this symmetry the relation

$$B_{40}^{C} = 14\, Dq \tag{17}$$

relates the experimental Dq to the crystal-field parameter B_{40}. The rotational invariant corresponding to equation (9) is given by

$$S_4(B) = \sqrt{B_{40}^2 + 2B_{43}^2} . \tag{18}$$

The approximate cubic field parameters corresponding to equation (10) are given by

$$B_{40}^{C} = \sqrt{\frac{7}{27}}\ S_4(B) , \tag{19}$$

$$B_{43}^{C} = \sqrt{\frac{10}{7}}\ B_{40}^{C} , \tag{20}$$

where we have used the result

$$S_4^{C}(B) = \sqrt{\frac{27}{7}}\ B_{40}^{C} . \tag{21}$$

In this cubic symmetry if $B_{40} < 0$, we have octahedral symmetry, and if $B_{40} > 0$, we have tetrahedral symmetry. The results given in equations (10), (12), (19), and (20) are sufficient for the ascent from C_4 and C_3 symmetry to cubic symmetry. Along with the relation

$$S_4(B) = \rho_4 S_4(A) , \tag{22}$$

we can determine the appropriate approximate cubic representation for a site in a solid provided we have detailed x-ray data on that solid. For particular solids where the site occupied by a transition-metal ion has low symmetry, such as C_2, the rotational invariant $S_2(A)$ can be used as well as $S_4(A)$ to approximate the site from a representation of higher symmetry. In section 4 the cubic approximation is considered for the

sites assumed to be occupied by quadruply ionized $5d^N$ transition-metal ions in each of the hosts considered.

The method we have chosen of obtaining approximate values of the $F^{(k)}$ and ρ_k values is to use the data obtained on the quadruply ionized ions of the $5d^N$ series (Re^{4+}, Os^{4+}, Ir^{4+}, and Pt^{4+}) (see table 28.3, p 133 of Morrison, 1989). These data were taken on the above four ions in Cs_2GeF_6 (Ge in O_h symmetry). From the x-ray data we obtain a point charge value A_{40} = 21,689 $cm^{-1}/(Å^4)$, and from the experimentally determined B_{40}, we obtain an average value of $\rho_4 = 3.108 \langle r^4 \rangle_{H-F}$. Using the $F^{(k)}$ (Morrison, 1989, table 2, p 12), we obtain an average value $F^{(k)} = 0.649\, F^{(k)}_{H-F}$. Using these values we obtain the results given in table 1 for the estimated parameters for the quadruply ionized ions of the $5d^N$ series. The values of ρ_2 used in constructing this table were obtained from $\rho_2 = 1.763 \langle r^2 \rangle_{H-F}$, as in Morrison and Turner (1988).

4. Cubic Approximation for Each Host

For each of the hosts given in the tables in appendix A, the appropriate cubic approximation is given below, using the monopole A_{nm} given in the appendix for that host.

4.1 $ZrSiO_4$

For the Zr site in $ZrSiO_4$ the monopole crystal-field components, A_{nm} ($cm^{-1}/Å^n$), are A_{20} = −12,756; A_{40} = 910.3; A_{44} = 8,630; and S_4 (A) = 12,239.

From equations (10) to (12), we have

$$B^C_{40} = 9347\, \rho_4 \ ,$$
$$B^C_{44} = 9347\, \rho_4 \sqrt{\frac{5}{14}} \ .$$

Since $A_{40} > 0$, we have chosen $B^C_{40} > 0$, and although the site symmetry is tetragonal (D_{2d}), the cubic approximation is octahedral. Actually for either octahedral or tetrahedral symmetry the relation $|A_{44}| \sim (5/14)^{1/2}|A_{40}|$ should prevail, which is obviously far from being a good approximation.

Using the values of ρ_n from table 1, we calculated the crystal-field parameters B_{nm} for W^{4+} ($5d^2$) in the cubic approximation and for the Zr

site in $ZrSiO_4$. The results are given in table 2a (cubic) and table 2b (Zr site). The parameters used in the calculation are given in each table. As can be seen, the energy levels are quite distinct and, in particular, the composition of the ground state is quite different—in the cubic approximation the ground state has 4 percent ^3P, which is completely missing in the D_{2d} symmetry. Furthermore, the ground state becomes almost pure ^3F (97 percent) in the D_{2d} symmetry. In both cases the spin-forbidden rule is invalid because of the admixture of the ^1D state into the Hund ground state by the strong spin-orbit interaction. Tables 2c and 2d present the cubic approximation and D_{2d} calculation, respectively, for Re^{4+} ($5d^3$) in the Zr site in $ZrSiO_4$. The results show that the cubic approximation is not good and in the analysis of experimental data, one should proceed directly from the D_{2d} analysis since the cubic approximation could be misleading.

4.2 $HfGeO_4$

For the Hf site in $HfGeO_4$ the monopole crystal-field components, A_{nm} ($cm^{-1}/Å^n$), are

$$A_{20} = 6465,\ A_{40} = -706.6,\ |A_{44}| = 4663, \text{ and } S_4(A) = 6632\ .$$

Then, as above,

$$B_{40}^C = -5056\,\rho_4\ ,$$
$$B_{44}^C = -5056\,\rho_4 \sqrt{\frac{5}{14}}\ .$$

With $A_{40} < 0$, we have tetrahedral symmetry. However, as in $ZrSiO_4$, the cubic representation is a poor one.

4.3 Li_2XTeO_6 (X = Zr, Hf)

For the Zr site in Li_2ZrTeO_6, the monopole crystal-field components ($cm^{-1}/Å^n$) are

$$A_{20} = 457,\ A_{40} = -14{,}546,\ |A_{43}| = 18{,}247, \text{ and } S_4(A) = 29{,}622\ .$$

From equations (17) and (18) we have

$$B_{40}^{C} = -15{,}083\ \rho_4\ ,$$
$$B_{43}^{C} = -15{,}083\ \rho_4 \sqrt{\frac{10}{7}}\ .$$

Since $B_{40}^{C} < 0$ in this cubic representation, the site is approximately octahedral. In this case $|A_{43}| \sim (10/7)^{1/2}\ |A_{40}|$, and the approximation is a good one. Also, because $A_{20} \sim 0$, the approximation is even better. However, since the oddfold fields A_{10}, A_{30}, A_{33}, A_{50}, and A_{53} are not negligible, the electric dipole transitions should be observable. We omit the details of the Hf site in Li_2HfTeO_6, since the results are very similar. However, since the spectra can be interpreted in terms of cubic symmetry and electric dipole transitions can be observed, this would probably be an excellent host.

To show the additional splitting in going from the cubic approximation to the correct symmetry in this host, we have used the above relation for the calculation of the energy levels of W^{4+} in the Zr site in this host. The results are given in tables 3a (cubic) and 3b (C_3). By comparing the results, we see that the reduction from cubic to C_3 for this host introduces what might be referred to as fine structure on the cubic field splittings. Thus, the assertion that the spectra can be interpreted in terms of the cubic approximation appears valid.

4.4 Li_6BeZrF_{12}

Li_6BeZrF_{12} is the only fluoride host, and judging from the results of $3d^N$ in fluoride hosts, the point-charge (monopole) model should be a good approximation. For the Zr site in Li_6BeZrF_{12}, the monopole crystal-field components, A_{nm} ($cm^{-1}/Å^n$), are

$$A_{20} = 1411,\ A_{40} = -3101,\ A_{44} = 5393,\ \text{and}\ S_4(A) = 9098\ .$$

From equations (10) to (12) we have

$$B_{40}^{C} = -6949\ \rho_4\ ,$$
$$B_{44}^{C} = -6949\ \rho_4 \sqrt{\frac{5}{14}}\ .$$

(Taking the value of B_{44} as positive or negative has no effect on the energy levels, just on the phase factors in the wave functions. However,

letting $B_{44} \rightarrow -B_{44}$ corresponds to a rotation of ±45°, and this rotation must be used in the evaluation of A_{32} and A_{52} in any crystal-field model.) Since the relation $|(A_{44})| \sim (5/14)^{1/2} |A_{40}|$, the cubic approximation can be used to advantage in the analysis of the experimental data. However, A_{20} is not negligible in this case, and its effects will probably be observable in the refinement of the experimental data. Li_6BeZrF_{12} is certainly a host material that should be further investigated.

4.5 $ZrGeO_2$

The crystal-field components for the Zr site in $ZrGeO_4$ are

$$A_{20} = 5{,}175;\ A_{40} = -6{,}023,\ |A_{44}| = 7{,}484;\ \text{and}\ S_4(A) = 12{,}178\ .$$

From equations (10) to (12), we have

$$B_{40}^C = -9301\ \rho_4\ ,$$
$$B_{44}^C = -9301\ \rho_4 \sqrt{\frac{5}{14}}\ .$$

However, since $(5/14)^{1/2}|A_{40}| = 3599$, we see that the cubic representation is not good (A_{44} is approximately twice this value). Nevertheless, a rough first interpretation of the experimental data in terms of the tetrahedral cubic group might be tried.

4.6 Zr_3GeO_8

Zr_3GeO_8 has two sites for the Zr ions, but when the crystal is doped with quadruply ionized $5d^N$ ions, these ions may go preferentially into one of the two sites. The crystal-field components for the Zr_1 site are

$$A_{20} = 10{,}659;\ A_{40} = -7{,}875;\ A_{44} = 6{,}875;\ \text{and}\ S_4(A) = 12{,}512\ .$$

For the cubic approximation we have

$$B_{40}^C = -9556\ \rho_4\ ,$$
$$B_{44}^C = -9556\ \rho_4 \sqrt{\frac{5}{14}}\ .$$

Again we have tetrahedral cubic symmetry but with the approximation rather poor: $A_{44} = -6875$, and $(5/14)^{1/2}|A_{40}| = 4706$. However, the

approximation is probably close enough to allow a first analysis of the experimental data.

For the Zr_2 site,

$$A_{20} = -7{,}440;\ A_{40} = -9{,}538;\ |A_{44}| = 8{,}910;\ \text{and}\ S_4(A) = 15{,}803\ .$$

These results give

$$B_{40}^{C} = -12{,}070\ \rho_4\ ,$$
$$B_{44}^{C} = -12{,}070\ \ \rho_4 \sqrt{\frac{5}{14}}\ .$$

As in the Zr_1 site, the tetrahedral cubic approximation is not very good but can be used in a preliminary analysis of the experimental data.

4.7 $ThSiO_4$

The crystal-field components for the Th site are

$$A_{20} = -6300,\ A_{40} = 18.45,\ A_{44} = 4906,\ \text{and}\ S_4(A) = 6938\ .$$

The cubic approximation is

$$B_{40}^{C} = 5299\ \rho_4\ ,$$
$$B_{44}^{C} = 5299\ \rho_4 \sqrt{\frac{5}{14}}\ .$$

However the cubic approximation is poor in this case and probably should not even be considered. For comparison with experimental data, on a particular ion, it would be better to use the parameters given in table 1 with the A_{nm} given above to calculate the energy levels.

4.8 $ThGeO_4$

For $ThGeO_4$, the same procedure as for $ThSiO_4$ applies for the zircon form, but for the scheelite form

$$A_{20} = 3593,\ A_{40} = -3236,\ |A_{44}| = 5405,\ \text{and}\ S_4(A) = 8301\ .$$

Then we have

$$B_{40}^{C} = -6340\,\rho_4 \ ,$$
$$B_{44}^{C} = -6340\,\rho_4\sqrt{\frac{5}{14}} \ .$$

Since we have $|A_{40}| < |A_{44}|$, the symmetry is far from cubic, but again in a crude analysis of the experimental data, the tetrahedral cubic symmetry may work.

5. Conclusion

X-ray data have been given on nine possible host materials for the quadruply ionized ions with the $4d^N$ and $5d^N$ electronic configurations. Very little information on the crystal growth and physical properties of host materials is given; however, some information can be found in the references to the x-ray data. For $ZrSiO_4$, several references are given to the crystal growth. The x-ray data were used to obtain the crystal-field components, and the reported data on several quadruply ionized ions with the $5d^N$ electronic configuration were used to approximate the crystal-field parameters for any quadruply ionized ion in that series. Cubic approximates were made for each host material and shown to be quite poor for some of the hosts. For W^{4+} ($5d^2$) in the Zr site in $ZrSiO_4$, explicit energy levels were calculated for the site in D_{2d} symmetry and for the cubic approximation. For comparison, a similar calculation was performed for Re^{4+} ($5d^3$). A second calculation made for W^{4+} in the Zr site in Li_2ZrTeO_6 with C_3 symmetry showed the effect of a small trigonal distortion at the site.

Approximate values necessary to calculate the energy levels of all the quadruply ionized ions with the $5d^N$ electronic configuration are given (table 1) even though the ionization state of some of the ions may be difficult if not impossible to achieve. No similar detailed calculations were done on the $4d^N$ because the data necessary for an approximate calculation were unavailable.

Table 1. Approximate free-ion parameters (cm^{-1}) and values of ρ_n ($Å^n$) for the quadruply ionized ions with the $5d^N$ configuration

Ion	nd^N	$F(2)$ B	$F(4)$ C	ρ_2	ρ_4
Ta	$5d^1$	— —	— —	1.732	5.757
W	$5d^2$	41,947 537.8	28,071 2,228	1.539	4.244
Re	$5d^3$	43,787 560.9	29,340 2,329	1.470	4.030
Os	$5d^4$	45,558 583.3	30,556 2,425	1.278	2.865
Ir	$5d^5$	47,364 606.0	31,804 2,524	1.206	2.530
Pt	$5d^6$	48,754 624.0	32,725 2,597	1.127	2.183
Au	$5d^7$	50,264 643.2	33,744 2,678	1.052	1.874
Hg	$5d^8$	51,795 662.8	34,778 2,760	0.9697	1.554
Tl	$5d^9$	— —	— —	0.8991	1.243

Table 2a. Energy levels of W^{4+} in the Zr site of $ZrSiO_4$, cubic approximation[a]

Level	I.R.[b]	Energy (cm^{-1})	Free ion state (%)
1	Γ_3	0	88 ^3F + 4 ^3P + 3 ^1D
2	Γ_5	471	84 ^3F + 8 ^3P + 6 ^1D
3	Γ_4	5,202	86 ^3F + 13 ^3P
4	Γ_1	6,243	70 ^3F + 21 ^3P + 4 ^1G
5	Γ_5	10,972	41 ^1D + 40 ^1G + 18 ^3F
6	Γ_3	11,829	45 ^1G + 43 ^1D + 7 ^3P
7	Γ_2	20,101	99 ^3F
8	Γ_1	21,013	33 ^1G + 30 ^1S + 21 ^3F
9	Γ_5	21,302	86 ^3F + 6 ^1G + 4 ^3P
10	Γ_4	22,239	91 ^3F + 4 ^3P + 3 ^1G
11	Γ_3	22,591	88 ^3F + 8 ^3P + 2 ^1G
12	Γ_4	27,406	80 ^3P + 14 ^3F + 4 ^1G
13	Γ_1	27,409	61 ^3P + 27 ^1G + 7 ^3F
14	Γ_5	27,930	41 ^3P + 33 ^1G + 15 ^1D
15	Γ_3	30,612	76 ^3P + 17 ^3F + 5 ^1G
16	Γ_5	32,666	46 ^3P + 30 ^1D + 15 ^1G
17	Γ_4	33,399	91 ^1G + 7 ^3F + 1 ^3P
18	Γ_5	42,252	93 ^3F + 3 ^1G + 2 ^1D
19	Γ_3	50,460	51 ^1D + 44 ^1G + 2 ^3P
20	Γ_1	61,007	61 ^1S + 35 ^1G + 2 ^3P

[a] *The parameters are $F^{(2)} = 41{,}947$; $F^{(4)} = 28{,}071$; $\zeta = 3{,}102$; $B_{40} = 39{,}669\ cm^{-1}$; and $B_{44} = (5/14)^{1/2} B_{40}$.*

[b] *Irreducible representations of the cubic T_d group (Koster et al, 1963).*

Table 2b. Energy levels of W^{4+} in the Zr site in $ZrSiO_4$[a]

Level	I.R.[b]	Energy (cm^{-1})	Free ion state (%)
1	Γ_3	0	97 ^3F + 2 ^1D
2	Γ_5	929	92 ^3F + 5 ^1D + 1 ^1G
3	Γ_1	2,917	80 ^3F + 12 ^1D + 5 ^1G
4	Γ_4	3,047	75 ^3F + 14 ^1D + 9 ^3P
5	Γ_2	7,295	98 ^3F
6	Γ_5	7,679	97 ^3F + 1 ^3P
7	Γ_3	8,358	93 ^3F + 4 ^3P + 2 ^1G
8	Γ_1	10,726	45 ^3P + 40 ^3F + 6 ^1S
9	Γ_4	10,831	43 ^3F + 41 ^1D + 13 ^3P
10	Γ_5	11,222	71 ^3F + 18 ^3P + 6 ^1D
11	Γ_1	12,106	41 ^1D + 28 ^1G + 19 ^3F
12	Γ_2	14,536	72 ^3P + 27 ^3F
13	Γ_5	14,634	37 ^3P + 29 ^1D + 17 ^3F
14	Γ_1	14,772	55 ^3F + 22 ^1G + 20 ^3P
15	Γ_3	14,975	50 ^3P + 27 ^3F + 12 ^1D
16	Γ_5	16,247	44 ^1G + 29 ^3F + 13 ^3P
17	Γ_4	17,044	60 ^1G + 15 ^3F + 15 ^3P
18	Γ_5	21,962	66 ^1G + 18 ^3F + 10 ^1D
19	Γ_1	21,992	75 ^1G + 14 ^3F + 6 ^3P
20	Γ_3	22,005	37 ^1D + 34 ^1G + 24 ^3F
21	Γ_4	23,169	34 ^1D + 34 ^1G + 19 ^3P
22	Γ_4	32,071	75 ^3F + 23 ^3P
23	Γ_1	32,443	46 ^1S + 23 ^3F + 16 ^1D
24	Γ_5	32,507	80 ^3F + 13 ^3P + 6 ^1G
25	Γ_3	34,991	47 ^3F + 31 ^3P + 17 ^1G
26	Γ_5	35,837	73 ^3P + 22 ^3F + 3 ^1G
27	Γ_1	35,894	63 ^3P + 14 ^3F + 11 ^1G
28	Γ_2	37,107	51 ^3F + 27 ^1G + 21 ^3P
29	Γ_4	39,165	79 ^3F + 18 ^3P + 1 ^1G
30	Γ_5	39,590	66 ^3F + 30 ^3P + 3 ^1G
31	Γ_1	40,269	52 ^3F + 44 ^3P + 1 ^1D
32	Γ_2	42,169	72 ^1G + 22 ^3F + 5 ^3P
33	Γ_3	44,998	44 ^1D + 37 ^1G + 9 ^3F
34	Γ_5	45,830	52 ^1G + 35 ^1D + 6 ^3P
35	Γ_1	74,204	42 ^1G + 35 ^1S + 20 ^1D

[a] *Parameters are $F^{(2)}$ = 41,947; $F^{(4)}$ = 28,071; ζ = 3,102; B_{20} = −19,631; B_{40} = 3,863; and B_{44} − 36,626 cm^{-1}.*

[b] *Irreducible representation of the tetragonal group, D_{2d}. Koster et al (1963).*

Table 2c. Energy levels of Re^{4+} in the Zr site in $ZrSiO_4$, cubic approximation[a]

Level	I.R.[b]	Energy (cm^{-1})	Free ion state (%)
1	Γ_8	0	89 ^4F + 3 $^2D1$ + 3 $^2D2$
2	Γ_8	9,397	25 ^2G + 20 ^4F + 16 ^2H
3	Γ_8	11,656	48 ^2G + 29 ^2H + 7 ^2P
4	Γ_6	12,804	33 ^2G + 24 ^2H + 23 ^2P
5	Γ_7	17,032	63 ^4F + 13 $^2D1$ + 8 ^2H
6	Γ_8	18,582	72 ^4F + 7 ^2G + 7 ^2H
7	Γ_8	20,027	73 ^4F + 9 ^2H + 7 ^4P
8	Γ_7	20,362	44 ^4F + 14 $^2D1$ + 13 ^2G
9	Γ_6	21,322	78 ^4F + 9 ^4P + 6 ^2P
10	Γ_8	22,457	27 ^4F + 21 ^2G + 20 ^2H
11	Γ_6	24,504	38 ^4P + 28 ^2G + 24 ^4F
12	Γ_8	26,505	45 ^4P + 22 ^2H + 15 ^4F
13	Γ_7	27,518	39 ^4F + 23 ^2H + 16 ^4P
14	Γ_8	28,717	42 ^4P + 39 ^4F + 9 ^2H
15	Γ_6	29,327	38 ^2G + 35 ^2H + 12 ^4P
16	Γ_8	30,583	30 ^2H + 19 ^4F + 16 ^2G
17	Γ_7	31,197	55 ^2G + 16 ^4P + 10 ^2H
18	Γ_6	32,498	52 ^2G + 21 ^4P + 15 ^2H
19	Γ_8	32,681	37 ^2H + 24 ^2G + 18 ^4F
20	Γ_8	35,005	28 ^2H + 27 $^2D2$ + 12 ^4F
21	Γ_6	36,207	29 ^2H + 28 ^2P + 23 ^2F
22	Γ_8	36,764	48 ^2H + 18 ^2F + 12 ^2G
23	Γ_7	37,755	31 ^2F + 20 $^2D2$ + 19 ^2H
24	Γ_8	39,768	35 ^2F + 28 $^2D2$ + 17 ^4P
25	Γ_7	41,848	95 ^2F + 1 ^2G + 1 $^2D2$
26	Γ_8	42,605	39 ^4F + 25 ^4P + 12 $^2D2$
27	Γ_7	42,770	36 ^4F + 34 ^4P + 16 ^2F
28	Γ_8	44,686	39 ^4F + 21 ^4P + 21 ^2F
29	Γ_6	45,627	57 ^4F + 17 ^2H + 14 ^4P
30	Γ_8	50,073	28 $^2D1$ + 23 ^2G + 20 $^2D2$

[a] *The parameters are $F^{(2)} = 43{,}787$; $F^{(4)} = 29{,}340$; $\zeta = 3{,}741$, $B_{40} = 37{,}668\ cm^{-1}$; and $B_{44} = (5/14)^{1/2} B_{40}$.*

[b] *Irreducible representations of the double cubic group, T_d (Koster et al, 1963).*

Table 2d. Energy levels of Re^{4+} in the Zr site of $ZrSiO_4$[a]

Level	I.R.[b]	Energy (cm^{-1})	Free ion state (%)
1	Γ_7	0	79 ^4F + 5 $^2D1$ + 5 $^2D2$
2	Γ_6	2,152	68 ^4F + 8 ^2G + 8 $^2D2$
3	Γ_7	5,444	87 ^4F + 8 ^4P + 1 $^2D2$
4	Γ_6	6,299	71 ^4F + 8 ^4P + 8 ^2G
5	Γ_6	8,399	67 ^4F + 12 ^4P + 9 ^2G
6	Γ_7	9,023	74 ^4F + 10 ^2G + 5 ^4P
7	Γ_6	10,683	31 ^2G + 29 ^4F + 22 ^2H
8	Γ_7	12,346	25 ^4P + 24 ^4F + 17 ^2P
9	Γ_7	13,289	51 ^2G + 33 ^2H + 5 ^4F
10	Γ_6	13,703	37 ^2H + 36 ^2G + 12 ^4F
11	Γ_7	14,337	45 ^2H + 43 ^2G + 4 $^2D2$
12	Γ_6	14,764	30 ^2G + 17 ^2H + 16 ^4P
13	Γ_6	18,666	26 ^4F + 23 ^4P + 21 ^2G
14	Γ_7	19,053	23 ^4F + 21 ^2H + 21 ^2G
15	Γ_6	19,848	27 ^2G + 24 ^2H + 19 ^4F
16	Γ_7	20,191	20 ^2H + 20 ^2G + 19 ^4P
17	Γ_6	21,395	28 ^2G + 27 ^2H + 12 ^2P
18	Γ_7	22,972	38 ^2G + 37 ^2H + 9 ^4F
19	Γ_6	23,777	30 ^2G + 24 ^2P + 17 ^2H
20	Γ_7	25,043	19 ^2H + 18 ^2F + 13 ^4F
21	Γ_6	26,288	26 ^2H + 19 ^4F + 18 ^2F
22	Γ_6	26,423	57 ^2H + 13 ^2F + 9 ^4F
23	Γ_7	26,682	27 $^2D2$ + 27 ^2H + 14 ^4F
24	Γ_7	27,662	32 ^4F + 28 ^2H + 15 ^2F
25	Γ_6	28,715	34 ^4F + 27 ^4P + 14 ^2F
26	Γ_7	29,226	38 ^4F + 17 ^2F + 16 ^4P
27	Γ_7	31,069	48 ^4F + 20 ^2F + 12 ^4P
28	Γ_6	31,233	67 ^4F + 10 ^2H + 8 ^4P
29	Γ_7	33,170	36 ^2F + 28 $^2D1$ + 13 ^4F
30	Γ_6	33,565	32 ^4P + 27 ^4F + 12 ^2H
31	Γ_7	34,774	75 ^4F + 7 ^4P + 6 ^2H
32	Γ_6	35,266	31 ^4F + 18 ^2G + 12 $^2D1$
33	Γ_6	36,297	45 ^4F + 13 $^2D1$ + 13 ^4P
34	Γ_6	37,827	31 ^4P + 25 ^4F + 16 ^2H
35	Γ_6	38,248	46 ^4F + 15 ^2H + 12 $^2D1$
36	Γ_7	38,303	39 ^4F + 20 ^4P + 12 ^2H
37	Γ_7	38,978	51 ^4P + 36 ^4F + 3 ^2H
38	Γ_6	39,715	30 ^2H + 18 ^4F + 17 ^4P
39	Γ_7	39,804	20 ^4P + 16 ^2H + 15 $^2D1$
40	Γ_7	40,583	66 ^4P + 12 ^4F + 8 ^2H
41	Γ_6	41,378	27 ^4P + 20 ^2H + 20 ^4F
42	Γ_7	42,564	25 ^2G + 19 ^2H + 16 ^2F
43	Γ_6	45,152	53 ^2H + 18 ^2G + 10 $^2D2$
44	Γ_7	45,917	33 $^2D2$ + 29 ^2G + 16 ^2H
45	Γ_6	46,436	28 ^2P + 26 ^2F + 20 ^4P
46	Γ_7	47,651	37 ^2H + 34 ^2F + 13 ^2G
47	Γ_6	48,165	40 ^2F + 30 ^2H + 14 ^2G
48	Γ_7	48,526	44 ^2F + 32 ^2H + 8 ^2G
49	Γ_7	49,045	42 ^2F + 27 ^2H + 19 ^2G
50	Γ_6	49,370	34 ^2F + 31 ^2H + 18 ^2G

[a] *The parameters are $F^{(2)} = 43,787$; $F^{(4)} = 29,340$; $\zeta = 3,741$; $B_{20} = -18,751$; $B_{40} = 3,669$; and $B_{44} = 34,779\ cm^{-1}$.*

[b] *Irreducible representation of the double D_{2d} group (Koster et al, 1963).*

Table 3a. Energy levels of W^{4+} in the Zr site in Li_2ZrTeO_6, cubic approximation[a]

Level	I.R.[b]	Energy (cm^{-1})	Free ion state (%)
1	Γ_3	0	83 ^3F + 11 ^3P + 3 ^1G
2	Γ_5	184	81 ^3F + 13 ^3P + 4 ^1D
3	Γ_4	4,362	82 ^3F + 17 ^3P
4	Γ_1	5,052	73 ^3F + 20 ^3P + 3 ^1S
5	Γ_4	10,778	50 ^1G + 42 ^1D + 6 ^3F
6	Γ_3	11,007	51 ^1G + 42 ^1D + 3 ^3F
7	Γ_1	22,265	47 ^1S + 44 ^1G + 8 ^3F
8	Γ_2	45,682	99 ^3F
9	Γ_5	46,344	96 ^3F + 2 ^3P + 1 ^1G
10	Γ_4	47,582	93 ^3F + 3 ^3P + 2 ^1G
11	Γ_3	47,618	90 ^3F + 8 ^3P
12	Γ_1	52,080	79 ^3P + 18 ^3F + 2 ^1G
13	Γ_4	52,909	76 ^3P + 17 ^3F + 5 ^1G
14	Γ_5	53,365	49 ^3P + 21 ^1G + 18 ^1D
15	Γ_3	55,652	76 ^3P + 22 ^3F + 1 ^1G
16	Γ_5	57,965	35 ^3P + 34 ^1D + 24 ^1G
17	Γ_4	58,884	91 ^1G + 5 ^3F + 2 ^3P

[a] *The parameters are $F^{(2)} = 41{,}947$; $F^{(4)} = 28{,}071$; $\zeta = 3{,}102$; $B_{40} = -64{,}012$; and $B_{43} = (10/7)^{1/2} B_{40}$ cm^{-1}.*

[b] *Irreducible representations of the cubic O group (Koster et al, 1963).*

Table 3b. Energy levels of W^{4+} in the Zr site in $LiZrTeO_6$[a]

Level	I.R.[b]	Energy (cm^{-1})	Free ion state (%)
1	Γ_1	0	82 ^3F + 13 ^3P + 3 ^1D
2	$\Gamma_{2,3}$	47	83 ^3F + 11 ^3P + 2 ^1D
3	$\Gamma_{2,3}$	788	80 ^3F + 12 ^3P + 4 ^1D
4	$\Gamma_{2,3}$	4,529	82 ^3F + 16 ^3P
5	Γ_1	5,065	82 ^3F + 17 ^3P
6	Γ_1	5,404	73 ^3F + 20 ^3P + 3 ^1S
7	$\Gamma_{2,3}$	10,360	50 ^1G + 41 ^1D + 6 ^3F
8	$\Gamma_{2,3}$	11,615	51 ^1G + 42 ^1D + 3 ^3F
9	Γ_1	11,732	51 ^1G + 42 ^1D + 5 ^3F
10	Γ_1	22,672	46 ^1S + 44 ^1G + 8 ^3F
11	Γ_1	45,897	99 ^3F
12	$\Gamma_{2,3}$	46,473	96 ^3F + 1 ^3P + 1 ^1G
13	Γ_1	46,680	94 ^3F + 4 ^3P + 1 ^1G
14	Γ_1	47,535	91 ^3F + 5 ^3P + 2 ^1G
15	$\Gamma_{2,3}$	47,776	90 ^3F + 7 ^3P + 1 ^1G
16	$\Gamma_{2,3}$	48,126	93 ^3F + 4 ^3P + 2 ^1G
17	Γ_1	52,319	78 ^3P + 18 ^3F + 2 ^1G
18	$\Gamma_{2,3}$	53,032	77 ^3P + 17 ^3F + 4 ^1G
19	Γ_1	53,452	45 ^3P + 23 ^1G + 19 ^1D
20	Γ_1	53,485	72 ^3P + 19 ^3F + 8 ^1G
21	$\Gamma_{2,3}$	53,769	49 ^3P + 22 ^1G + 17 ^1D
22	$\Gamma_{2,3}$	55,982	76 ^3P + 22 ^3F + 1 ^1G
23	Γ_1	58,009	38 ^3P + 32 ^1D + 21 ^1G
24	$\Gamma_{2,3}$	58,239	33 ^3P + 30 ^1G + 29 ^1D
25	Γ_1	58,821	88 ^1G + 6 ^3F + 4 ^3P
26	$\Gamma_{2,3}$	59,530	85 ^1G + 5 ^1D + 4 ^3F

[a] *The parameters are $F^{(2)} = 41{,}947$; $F^{(4)} = 28{,}071$; $\zeta = 3{,}102$; $B_{20} = 703.2$; $B_{40} = -61{,}733$; and $B_{43} = 77{,}440\ cm^{-1}$.*

[b] *Irreducible representations of the C_3 group (Koster et al, 1963) ($\Gamma_{2,3} = \Gamma_2 + \Gamma_3$).*

References

Ballhausen, C. J. (1962), *Introduction to ligand field theory*, McGraw-Hill, New York, pp 273–292.

Di Gregario, S., M. Greenblatt, J. H. Pifer, and M. D. Sturge (1982), An ESR and optical study of V^{4+} in zircon-type crystals, J. Chem. Phys. **76**, 2931.

Koster, G. F., J. O. Dimmock, R. G. Wheeler, and H. Statz (1963), *Properties of the Thirty-Two Point Groups*, MIT Press, Cambridge, MA.

Morrison, C. A. (September 1989), Host materials for transition-metal ions, Harry Diamond Laboratories, HDL-DS-89-1. (Reported data on $4d^N$ and $5d^N$ ions are given in sections 13, 21, 28, 31, 33, and 35.)

Morrison, C. A. (1988), Angular momentum theory applied to interactions in solids, Lecture Notes in Chemistry **47**, Springer-Verlag, New York.

Morrison, C. A., and G. A. Turner (October 1988), Analysis of the optical spectra of triply ionized transition-metal ions in yttrium aluminum garnet (YAG), Harry Diamond Laboratories, HDL-TR-2150.

Nielson, C. W. and G. F. Koster (1963), *Spectroscopic Coefficients for p^n, d^n, and f^n Configurations*, MIT Press, Cambridge, MA.

Appendix A.—Detailed X-Ray Data on 10 Host Materials

Appendix A

Contents

Page

A-1. $ZrSiO_4$ 28

A-2. $HfGeO_4$ 31

A-3. Li_2XTeO_6 33

A-4. Li_6BeZrF_{12} 35

A-5. $ZrGeO_4$ 36

A-6. Zr_3GeO_8 38

A-7. $ThSiO_4$ 40

A-8. $ThGeO_4$ 42

Appendix A

The following tables give the crystallographic and x-ray data on each of the 10 host materials discussed in the main body of text. The crystal-field components, A_{nm}, are calculated for the monopole (point charge), self-induced, and dipole contributions. Following each table is a list of references for that particular compound. These references include such topics as crystal growth, index of refraction, and electron spin resonance investigations. However, these reference lists are not, in any sense, extensive, and if further investigations are contemplated on any compound, additional literature searches should be undertaken.

Appendix A

A-1. $ZrSiO_4$

A-1.1 Crystallographic data on $ZrSiO_4$

Tetragonal D_{4h}^{19} ($4_1/amd$), 141 (second setting)

Ion	Site	Symmetry	x	y	z	q	α (Å^3)
Zr	4*a*	D_{2d}	0	3/4	1/8	4	0.48[a]
Si	4*b*	D_{2d}	0	1/4	3/8	4	0.03[a]
O	16*h*	C_s	0	y	z	−2	1.349[b]

[a] *Fraga et al (1976).*
[b] *Schmidt et al (1979).*

A-1.2 X-ray data

a (Å)	c (Å)	y	z	Ref.
6.6164	6.0150	0.067	0.198	*a*
6.607	5.982	0.0661	0.1953	*b*

[a] *Wyckoff (1968).*
[b] *Robinson et al (1971).*

A-1.3 Crystal-field components, A_{nm} (cm^{-1}/Å^n), for Zr (D_{2d}) site (x-ray data of Wyckoff)

A_{nm}	Monopole	Self-induced	Dipole	Total
A_{20}	−12,765	349.4	33,644	21,229
A_{32}	−1,332	449.2	958.9	76.55
A_{40}	910.3	−1,130	524.3	304.5
A_{44}	8,630	−2,943	−7,031	−1,344
A_{52}	6,142	−2,379	−1,796	1,967

A-1.4 Crystal-field components, A_{nm} (cm^{-1}/Å^n), for Zr (D_{2d}) site (Robinson et al data)

A_{nm}	Monopole	Self-induced	Dipole	Total
A_{20}	−13,840	388.8	34,843	21,392
A_{32}	−522.2	332.7	754.3	564.8
A_{40}	826.4	−1,175	369.0	20.10
A_{44}	9,024	−3,114	−7,316	-1,406
A_{52}	6,357	−2,514	−1.703	2,142

A-1.5 $ZrSiO_4$ (zircon) references

Caruba, R., A. Baumer, and P. Hartman (1988), Crystal growth of synthetic zircon round natural seeds, J. Cryst. Growth **88,** 297.

Di Gregario, S., M. Greenblatt, and J. H. Pifer (1980), ESR of Nb^{4+} in zircon, Stat. Sol. **(b)101,** K149.

Di Gregario, S., M. Greenblatt, J. H. Pifer, and M. D. Sturge (1982), An ESR and optical study of V^{4+} in zircon-type crystals, J. Chem. Phys. **76,** 2931.

Fraga, S., J. Karwowski, and K. M. S. Saxena (1976), *Handbook of Atomic Data*, **5,** 319.

Harris, E. A., J. H. Mellor, and S. Parke (1984), Electron paramagnetic resonance of tetravalent praseodymium in zircon, Phys. Stat. Sol. **(b)122,** 757.

Hong Xiaoyu, Bai Gui-ru, and Zhao Min-guang (1985), The study of the optical and the EPR spectra of V^{4+} in zircon-type crystals, J. Phys. Chem Solids **46,** 719.

Koster, G. F., J. O. Dimmock, R. G. Wheeler, and H. Statz (1963), *Properties of the Thirty-Two Point Groups*, MIT Press, Cambridge, MA.

Kusabu, K., T. Yagi, M. Kikuchi, and Y. Syono (1986), Structural considerations on the mechanism of the shock-induced zircon-scheelite transition in $ZrSiO_4$, J. Phys. Chem. Solids **47,** 675.

Lyons, K. B., M. D. Sturge, and M. Greenblatt (1984), Low-frequency Raman spectrum of $ZrSiO_4$:V^{4+}: An impurity-induced dynamical distortion, Phys. Rev. **B30,** 2127.

Newman, D. J., and B. Ng (1989), Crystal-field superposition model analysis for tetravalent actinides, J. Phys: Condens. Mater. **1,** 1613.

Poirot, I. S., W. K. Kot, N. M. Edelstein, M. M. Abraham, C. B. Finch, and L. A. Biatner (1989), Optical study and analysis of Pu^{4+} in single crystals of $ZrSiO_4$, Phys. Rev. **B39,** 6388.

Poirot, I. S., W. K. Kot, G. Shallimoff, N. M. Edelstein, M. M. Abraham, C. B. Finch, and L. A. Boatner (1988), Optical and E. P. R. investigations of Np^{4+} in single crystals of $ZrSiO_4$, Phys. Rev. **B37,** 3255.

Robinson, K., G. V. Gibbs, and P. H. Ribbe (1971), The structure of zircon: A comparison with garnet, Amer. Mineral. **56,** 782.

Schmidt, P. C., A. Weiss, and T. P. Das (1979), Effects of crystal-fields and self-consistency on dipole and quadruple polarization of closed shell ions, Phys. Rev. **B19,** 5525.

Silich, L. M., E. M. Kurpan, N. M. Bobkora, A. A. Stepanchuk, and S. A. Gailevich (1988), Quantitative x-ray phase analysis of ceramic in the Al_2O_3–TiO_2 system with AlO_2 and $ZrSiO_4$ added, Neorg. Mater. **24,** 1196.

Wyckoff, R. W. G. (1968), *Crystal Structures*, **4,** 157.

A-2 $HfGeO_4$

A-2.1 Crystallographic data on $HfGeO_4$

Tetragonal C_{4h}^5 ($I4_1/a$), 88 (first setting), $Z = 4$

Ion	Site	Symmetry	x	y	z	q	α (Å^3)[b]
Hf	4*b*	S_4	0	0	1/2	4	0.57[a]
Ge	4*a*	S_4	0	0	0	4	0.12[a]
O	16*f*	C_1	x	y	z	−2	1.349[b]

[a] *Fraga et al (1976).*
[b] *Schmidt et al (1979).*

A-2.2 X-ray data on $HfGeO_4$

a (Å)	c (Å)	x	y	z
4.849[a]	10.50	0.25	0.11	0.07
4.862[b]	10.497	0.2678	0.1739	0.0831

[a] *Wyckoff (1968).*
[b] *Ennaciri et al (1986).*

A-2.3 Lattice sum, A_{nm} (cm^{-1}/Å^n), for Hf site (S_4) (Wyckoff, 1968)

A_{nm}	Monopole	Self-induced	Dipole	Total
A_{20}	6,465	−662.8	−13,794	−7,992
ReA_{32}	3,527	−434.0	4,855	7,948
ImA_{32}	512.3	−45.50	674.9	1,141
A_{40}	−706.6	389.5	3,039	2,721
ReA_{44}	−2,525	755.7	139.9	−1,629
ImA_{44}	−3,920	961.5	2,154	−804.2
ReA_{52}	3,026	−966.8	−90[illegible].1	1,155
ImA_{52}	−3,758	1,289	2,735	267.2
$\|A_{44}\|$	4,663	—	—	1,817

A-2.4 $HfGeO_4$ references

Ennaciri, A., A. Kahn, and D. Michel (1986), Crystal structures of $HfGeO_4$ and $ThGeO_4$ germanates, J. Less-Common Metals, **124**, 105.

Fraga, S., J. Karwowski, and K. M. S. Saxena (1976), *Handbook of Atomic Data*, **5**, 319.

Schmidt, P. C., A. Weiss, and T. P. Das (1979), Effects of crystal-fields and self-consistency on dipole and quadrupole polarization of closed shell ions, Phys. Rev. **B19,** 5525.

Wyckoff, R. W. G. (1968), *Crystal Structures*, **3**, Interscience, New York, 21.

A-3. Li_2XTeO_6 (X = Zr, Hf)

A-3.1 Crystallographic data on Li_2XTeO_6 (X = Zr, Hf)

Trigonal C_3^4 ($R3$), 146 (hexagonal setting), $Z = 3$

Ion	Site	Symmetry	x	y	z	q	1.349[a]
Li1	3*a*	C_3	0	0	z	1	0.0321[a]
Li2	3*a*	C_3	0	0	z	1	0.0321[a]
X	3*a*	C_3	0	0	z	4	α_X[b]
Te	3*a*	C_3	0	0	z	6	0.20[b]
O1	9*b*	C_1	x	y	z	−2	1.349[a]
O2	9*b*	C_1	x	y	z	−2	1.349[a]

[a] *Schmidt et al (1979).*
[b] *Fraga et al (1976).*

A-3.2 X-ray data[a]

X	a (Å)	c (Å)	z_{Li1}	z_{Li2}	z_x	z_{Te}	x_{O1}	y_{O1}	z_{O1}
Zr	5.172	13.847	0.29	0.76	0.993	0.500	0.049	0.355	0.077
Hf	5.164	13.782	—	—	—	—	—	—	—

X	x_{O2}	y_{O2}	z_{O2}	α_X (Å^3)
Zr	0.652	0.962	0.576	0.48
Hf	—	—	—	0.57

[a] *Choisnet et al (1988).*

A-3.3 Lattice sum, A_{nm} (cm^{-1}/Å^n), for Zr site (C_3)

A_{nm}	Monopole	Self-induced	Dipole	Total
A_{10}	−16,240	—	−5,318	−21,557
A_{20}	457.0	26.77	5,159	5,643
A_{30}	2,319	−971.7	5,941	7,289
ReA_{33}	1,582	−239.1	−5,242	−3,899
ImA_{33}	−2,633	881.9	−4,924	−6,675
A_{40}	−14,546	5,506	467.2	−8,573
ReA_{43}	3,925	−1,773	9,713	11,865
ImA_{43}	17,820	−6,293	−4,997	6,530
A_{50}	1,239	−610.4	−828.5	−200.1
ReA_{53}	451.4	−38.55	−1,981	−1,568
ImA_{53}	−1,805	1,241	−958.1	−1,522
$\lvert A_{43}\rvert$	18,247	—	—	13,543

A-3.4 Lattice sum, A_{nm} ($cm^{-1}/Å^n$), for Hf site (C_3). [The positions of the ions within the unit cell are those of Li_2ZrTeO_6.]

A_{nm}	Monopole	Self-induced	Dipole	Total
A_{10}	68,052	—	9,798	77,850
A_{20}	251.1	55.40	7,418	7,724
A_{30}	2,387	-998.3	-28,186	-26,797
ReA_{33}	1,607	-243.4	1,478	2,842
ImA_{33}	-2,677	903.0	21,103	19,330
A_{40}	-14,696	5,605	3,543	-5,548
ReA_{43}	3,972	-1,811	11,185	13,345
ImA_{43}	18,073	-6,432	-9,130	2,511
A_{50}	1,249	-617.3	4,789	5,421
ReA_{53}	453.8	-38.22	-1,007	-591.8
ImA_{53}	-1,834	1,270	4,337	3,773
$\|A_{43}\|$	18,504	—	—	13,579

A-3.5 Li_2ZrTeO_6 references

Choisnet, J., A. Rulmont, and P. Tarte (1988), Les tellurates mixtes Li_2ZrTeO_6 et Li_2HfTeO_6: un nouveau phénomène d'ordre dans la famille corindou, J. Solid State Chem. **75**, 124.

Fraga, S., J. Karwowski, and K. M. S. Saxena (1976), *Handbook of Atomic Data*, **5**, 319.

Schmidt, P. C., A. Weiss, and T. P. Das (1979), Effects of crystal-fields and self-consistency on dipole and quadrupole polarization of closed shell ions, Phys. Rev. **B19**, 5525.

A-4. Li_6BeZrF_{12}

A-4.1 Crystallographic data on Li_6BeZrF_{12}

Tetragonal D_{4h}^{19} ($I4_1/amd$), 141 (second setting), $Z = 4$

Ion	Site	Symmetry	x^a	y	z	q	α (Å^3)^b
Be	4*a*	D_{2d}	0	3/4	1/8	2	0.0125
Zr	4*b*	D_{2d}	0	1/4	3/8	4	0.480
Li_1	8*e*	C_{2v}	0	1/4	0.1034	1	0.0321
Li_2	16*f*	C_2	0.2303	0	0	1	0.0321
F_1	16*h*	C_s	0	0.5340	0.4207	−1	0.731
F_2	16*h*	C_s	0	0.0260	0.2903	−1	0.731
F_3	16*h*	C_s	0	−0.0568	0.0745	−1	0.731

[a] *X-ray data: a = 6.570, c = 18.62, Wyckoff (1968).*

[b] *Schmidt et al (1979) except for Zr which is from Fraga et al (1976).*

A-4.2 Crystal-field components, A_{nm} (cm^{-1}/Å^n), for Zr (D_{2d}) site

A_{nm}	Monopole	Self-induced	Dipole	Total
A_{20}	1,411	97.22	−6,180	−4,672
A_{32}	−3,101	763.4	−4,360	−6,697
A_{40}	−4,960	1,762	−2,039	−5,237
A_{44}	5,393	−1,943	3,955	7,405
A_{52}	3,606	−1,754	2,452	4,304

A-4.3 Li_6BeZrF_{12} references

Fraga, S., J. Karwowski, and K. M. S. Saxena (1976), *Handbook of Atomic Data*, **5**, 319.

Schmidt, P. C., A. Weiss, and T. P. Das (1979), Effects of crystal-fields and self-consistency on dipole and quadrupole polarization of closed shell ions, Phys. Rev. **B19,** 5525.

Wyckoff, R. W. G. (1968), *Crystal Structures*, Vol. **4**, Interscience, New York, 57.

Appendix A

A-5. $ZrGeO_4$

A-5.1 Crystallographic data on $ZrGeO_4$

Tetragonal C_{4h}^6 ($I4_1/a$), 88 (first setting), $Z = 4$

Ion	Site	Symmetry	x^a	y	z	q	G [illegible]^b
Ge	4*a*	S_4	0	0	0	4	[illegible]
Zr	4*b*	S_4	0	0	1/2	4	[illegible]
O	16*f*	C_1	x	y	z	−2	1

[a] *X-ray data: $a = 4.8660$, $c = 10.55$ (Å), $x = 0.2664$, $y = 0.1726$, $z = 0.0822$ (Ennaciri et al, 1984).*
[b] *Fraga et al (1976).*

A-5.2 Crystal-field components, A_{nm} ($cm^{-1}/Å^n$), for Zr (S_4) site

A_{nm}	Monopole	Self-induced	Dipole	Total
A_{20}	5,175	−202	−13,444	−8,470
ReA_{32}	−2,584	543	3,702	1,661
ImA_{32}	5,083	−1,228	2,074	5,928
A_{40}	−6,023	1,773	7,119	2,870
ReA_{44}	−5,668	1,928	−154	−3,894
ImA_{44}	−4,887	1,457	50	−3,380
ReA_{52}	1,982	−754	394	1,622
ImA_{52}	−5,705	2,280	717	−2,708
$\|A_{44}\|$	7,484	—	—	5,516

A-5.3 Crystal-field components, A_{nm} ($cm^{-1}/Å^n$), for Ge (S_4) site in $ZrGeO_4$

A_{nm}	Monopole	Self-induced	Dipole	Total
A_{20}	−16,423	2,648	−17,512	−31,288
ReA_{32}	17,821	−5,603	8,684	20,902
ImA_{32}	36,558	−12,128	21,800	46,235
A_{40}	−16,132	7,646	−3,565	−12,051
ReA_{44}	−10,322	5,533	−6,628	−11,417
ImA_{44}	12,115	−6,078	9,726	15,764
ReA_{52}	−2,489	1,770	−3,199	−3,918
ImA_{52}	−5,540	3,989	−6,510	−8,062
$\|A_{44}\|$	15,916	—	—	19,464

A-5.4 $ZrGeO_4$ references

Ennaciri, A., A. Kahn, and D. Michel (1986), Crystal structures of $HfGeO_4$ and $ThGeO_4$ germanates, J. Less-Common Metals, **124**, 105.

Fraga, S., J. Karwowski, and K. M. S. Saxena (1976), *Handbook of Atomic Data*, **5**, 319.

Schmidt, P. C., A. Weiss, and T. P. Das (1979), Effects of crystal-fields and self-consistency on dipole and quadrupole polarization of closed shell ions, Phys. Rev. **B19,** 5525.

Appendix A

A-6. Zr_3GeO_8

A-6.1 Crystallographic data on Zr_3GeO_8

Tetragonal D_{2d}^{11} ($1\bar{4}2m$), 121 (first setting), $Z = 2$

Ion	Site	Symmetry	x[a]	y	z	q	α (Å^3)[b]
Ge	2*a*	D_{2d}	0	0	0	4	0.12[b]
Zr_1	2*b*	D_{2d}	0	0	1/2	4	0.48[b]
Zr_2	4*d*	S_4	0	1/2	1/4	4	0.48[b]
O_1	8*i*	C_s	0.2004	0.2004	0.3410	−2	1.349[c]
O_2	8*i*	C_s	0.2170	0.2170	0.0904	−2	1.349[c]

[a] *X-ray data: a = 5.005, c = 10.550 (Å), Ennaciri et al (1984).*
[b] *Fraga et al (1976).*
[c] *Schmidt et al (1979).*

A-6.2 Crystal-field components, A_{nm} (cm^{-1}/Å^n), for Ge (D_{2d}) site

A_{nm}	Monopole	Self-induced	Dipole	Total
A_{20}	−9,412	1,462	−13,999	−21,949
A_{32}	37,705	−11,897	26,755	52,564
A_{40}	−17,256	7,914	−7,401	−16,742
A_{44}	13,709	−6,580	10,516	−17,644
A_{52}	−3,458	2,382	−5,316	−6,393

A-6.3 Crystal-field components, A_{nm} (cm^{-1}/Å^n), for Zr_1 (D_{2d}) site

A_{nm}	Monopole	Self-induced	Dipole	Total
A_{20}	10,659	−900	−7,933	1,827
A_{32}	300.1	38.3	−98.4	240.6
A_{40}	−7,875	2,384	6,546	1,055
A_{44}	6,875	−2,024	−91.5	4,760
A_{52}	−5,795	2,320	−289.0	−3,764

A-6.4 Crystal-field components, A_{nm} ($cm^{-1}/Å^n$), for Zr_2 (S_4) site of Zr_3GeO_8

A_{nm}	Monopole	Self-induced	Dipole	Total
A_{20}	-7,440	974	-6,987	-13,453
ReA_{32}	-6,953	1,611	129	-5,219
ImA_{32}	-12,700	3,350	-5,948	-15,298
A_{40}	-9,538	2,874	3,317	-3,347
ReA_{44}	-6,213	2,229	-170	-4,154
ImA_{44}	6,389	-2,090	2,204	6,500
ReA_{52}	1,489	-645	1,029	1,873
ImA_{52}	3,755	-1,660	1,473	3,568
$\lvert A_{44}\rvert$	8,910	—	—	7,714

A-6.5 Zr_3GeO_8 references

Ennaciri, A., A. Kahn, and D. Michel (1986), Crystal structures of $HfGeO_4$ and $ThGeO_4$ germanates, J. Less-Common Metals, **124**, 105.

Fraga, S., J. Karwowski, and K. M. S. Saxena (1976), *Handbook of Atomic Data*, **5**, 319.

Schmidt, P. C., A. Weiss, and T. P. Das (1979), Effects of crystal-fields and self-consistency on dipole and quadrupole polarization of closed shell ions, Phys. Rev. **B19**, 5525.

Appendix A

A-7. $ThSiO_4$

A-7.1 Crystallographic data on $ThSiO_4$

Tetragonal D_{4h}^{19} ($I4_1/amd$), 141 (first setting), $Z = 4$

Ion	Site	Symmetry	x^a	y	z	q	α (Å^3)
Th	4*a*	D_{2d}	0	3/4	1/8	4	1.52[b]
Si	4*b*	D_{2d}	0	3/4	5/8	4	0.030[b]
O	16*h*	C_s	0	0.0732	0.2104	−2	1.349[c]

[a] *X-ray data: a = 7.1328 Å, c = 6.3188 Å, Taylor et al (1978).*
[b] *Fraga et al (1976).*
[c] *Schmidt et al (1979).*

A-7.2 Crystal-field components, A_{nm} (cm^{-1}/Å^n), for Th site (D_{2d})

A_{nm}	Monopole	Self-induced	Dipole	Total
A_{20}	−6,300	−141.4	26,500	20,058
A_{32}	−1,653	193.5	1,666	206.2
A_{40}	18.45	−493.3	1,350	875.4
A_{44}	4,906	−1,316	−4,142	−552.9
A_{52}	3,753	−1,108	−1,116	1,529

A-7.3 Crystal-field components, A_{nm} (cm^{-1}/Å^n), for Si site (D_{2d})

A_{nm}	Monopole	Self-induced	Dipole	Total
A_{20}	7,634	−3,788	28,562	32,408
A_{32}	−64,599	24,940	−45,571	−85,230
A_{40}	−35,517	21,569	−31,618	−46,566
A_{44}	13,907	−9,471	10,306	14,741
A_{52}	−7,113	6,834	−14,295	−14,573

A-7.4 $ThSiO_4$ references

Fraga, S., J. Karwowski, and K. M. S. Saxena (1976), *Handbook of Atomic Data*, **5**, 319.

Schmidt, P. C., A. Weiss, and T. P. Das (1979), Effects of crystal-fields and self-consistency on dipole and quadrupole polarization of closed shell ions, Phys. Rev. **B19,** 5525.

Taylor, M., and R. C. Ewing (1978), The crystal structures of the $ThSiO_4$ polymorphs: Huttonite and Thorite, Acta. Crystal. **B34,** 1074.

Appendix A

A-8. $ThGeO_4$

A-8.1 Crystallographic data on $ThGeO_4$

Tetragonal D_{4h}^{19} ($I4_1/amd$), 141 (first setting), $Z = 4$

Ion	Site	Symmetry	x	y	z	q	α (Å^3)
Th	4*a*	D_{2d}	0	0	0	4	1.52[b]
Ge	4*b*	D_{2d}	0	0	1/2	4	0.12[b]
O	16*h*	C_s	0	0.1803[a]	0.3214	–2	1.349[c]

[a] *X-ray data: a = 7.230 Å, c = 6.539 Å, Ennaciri et al (1986).*
[b] *Fraga et al (1976).*
[c] *Schmidt et al (1979).*

A-8.2 Tetragonal C_{4h}^6 ($I4_1/a$), 88 (first setting), $Z = 4$

Ion	Site	Symmetry	x	y	z	q	α (Å^3)
Th	4*b*	S_4	0	0	1/2	4	1.52[b]
Ge	4*b*	S_4	0	0	0	4	0.12[b]
O	16*f*	C_1	0.2548[a]	0.1493	0.0787	–2	1.348[c]

[a] *X-ray data: a = 5.145 Å, c = 10.531 Å, Ennaciri et al (1986).*
[b] *Fraga et al (1976).*
[c] *Schmidt et al (1979).*

A-8.3 Crystal-field components, A_{nm} (cm^{-1}/Å^n), for Th site (D_{2d})

A_{nm}	Monopole	Self-induced	Dipole	Total
A_{20}	–8,188	49.52	21,620	13,482
A_{32}	151.6	–68.33	171.6	254.8
A_{40}	549.2	–547.2	448.5	450.6
A_{44}	5,368	–1,397	–3,701	270.1
A_{52}	–3,634	1,074	829.8	–1,730

A-8.4 Crystal-field components, A_{nm} (cm^{-1}/Å^n), for Ge site (D_{2d})

A_{nm}	Monopole	Self-induced	Dipole	Total
A_{20}	15,677	−3,858	19,380	31,119
A_{32}	48,087	−15,117	27,015	59,985
A_{40}	−26,107	12,492	−17,436	−31,051
A_{44}	8,289	−4,775	5,642	9,156
A_{52}	7,228	−5.656	8,759	10,331

A-8.5 Crystal-field components, A_{nm} (cm^{-1}/Å^n), for Th site (S_4)

A_{nm}	Monopole	Self-induced	Dipole	Total
A_{20}	3,593	−382.9	−4,985	−1,775
ReA_{32}	1,850	−150.2	3,916	5,616
ImA_{32}	−98.96	33.57	124.6	59.21
A_{40}	−3,236	977.3	3,822	1,563
ReA_{44}	−3,857	977.1	1,069	−1,811
ImA_{44}	−3,787	888.8	810.3	−2,088
ReA_{52}	1,923	−599.4	138.0	1,461
ImA_{52}	−3,970	1,326	1,369	−1,275
$\lvert A_{44}\rvert$	5,405	—	—	2,764

A-8.6 Crystal-field components, A_{nm} (cm^{-1}/Å^n), for Ge site (S_4)

A_{nm}	Monopole	Self-induced	Dipole	Total
A_{20}	−21,877	3,538	−13,762	−32,101
ReA_{32}	22,842	−7,897	15,609	30,554
ImA_{32}	40,279	−13,830	23,195	49,644
A_{40}	−16,030	8,434	−7,823	−15,419
ReA_{44}	−9,474	5,340	−3,575	−7,709
ImA_{44}	16,075	−8,588	13,046	20,533
ReA_{52}	−3,667	2,846	−4,027	−4,849
ImA_{52}	−6,414	5,096	−5,729	−7,048
$\lvert A_{44}\rvert$	18,659	—	—	21,932

A-8.7 $ThGeO_4$ references

Ennaciri, A., A. Kahn, and D. Michel (1986), Crystal structures of $HfGeO_4$ and $ThGeO_4$ germanates, J. Less-Common Metals, **124**, 105.

Fraga, S., J. Karwowski, and K. M. S. Saxena (1976), *Handbook of Atomic Data*, **5**, 319.

Schmidt, P. C., A. Weiss, and T. P. Das (1979), Effects of crystal-fields and self-consistency on dipole and quadrupole polarization of closed shell ions, Phys. Rev. **B19,** 5525.

Distribution

Administrator
Defense Technical Information Center
Attn DTIC-DDA (2 copies)
Cameron Station, Bulding 5
Alexandria, VA 22304-6145

Director
Night Vision & Electro-Optics Laboratory
Attn Technical Library
Attn R. Buser
Attn A. Pinto (2 copies)
Attn J. Hebersat
Attn R. Rhode
Attn W. Tressel
Ft Belvoir, VA 22060

Director
Defense Advanced Research Projects Agency
Attn J. Friebele
1400 Wilson Blvd
Arlington, VA 22290

Director
Defense Nuclear Agency
Attn Tech Library
Washington, DC 20305

Under Secretary of Defense Res & Engineering
Attn Tech Library, 3C128
Washington, DC 20301

Office of the Deputy Chief of Staff for Research, Development, & Acquisition
Department of the Army
Attn DAMA-ARZ-B,
I. R./ Hershner
Washington, DC 20310

Commander
US Army Armament Munitions & Chemical Command (AMCCOM) R&D Center
Attn DRDAR-TSS, STINFO Div
Dover, NJ 07801

Commander
Atmospheric Sciences Laboratory
Attn Technical Library
White Sands Missile Range, NM 88002

Director
US Army Ballistic Research Laboratory
Attn SLCBR-DD-T (STINFO)
Aberdeen Proving Ground, MD 21005

Director
US Army Electronics Warfare Laboratory
Attn J. Charlton
Attn DELET-DD
Ft Monmouth, NJ 07703

Commanding Officer
USA Foreign Science & Technology Center
Attn DRXST-BS, Basic Science Div
Federal Office Building
Charlottesville, VA 22901

Commander
US Army Materials & Mechanics Research Center
Attn DRXMR-TL, Tech Library
Watertown, MA 02172

US Army Materiel Systems Analysis Activity
Attn DRXSY-MP, Library
Aberdeen Proving Ground, MD 21005

Commander
US Army Missile & Munitions Center & School
Attn ATSK-CTD-F
Attn DRDMI-TB, Redstone Sci Info Center
Redstone Arsenal, AL 35809

Commander
US Army Research Office Durham
Attn R. J. Lontz
Attn M. Stosio
Attn M. Ciftan
Attn R. Guenther
Attn C. Bogosian
Research Triangle Park, NC 27709

Commander
USA Rsch & Std Gp (Europe)
Attn Chief, Physics & Math Branch
FPO, New York 09510

Distribution (cont'd)

Commander
US Army Test & Evaluation Command
Attn D. H. Sliney
Attn Tech Library
Aberdeen Proving Ground, MD 21005

Commander
US Army Troop Support Command
Attn DRXRES-RTL, Tech Library
Natick, MA 01762

Office of Naval Research
Attn J. Murday
Arlington, VA 22217

Director
Naval Research Laboratory
Attn Code 5554, R. E. Allen
Attn Code 2620, Tech Library Br
Attn G. Quarles
Attn G. Kintz
Attn A. Rosenbaum
Attn G. Risenblatt
Attn Code 5554, F. Bartoli
Attn Code 6540, S. R. Bowman
Attn Code 5554, L. Esterowitz
Washington, DC 20375

Commander
Naval Weapons Center
Attn Code 3854, R. Schwartz
Attn Code 3854, M. Hills
Attn Code 3854, M. Nadler
Attn Code 3854, R. L. Atkins
Attn DOCE 343, Technical Information Department
China Lake, CA 93555

Air Force Office of Scientific Research
Attn Major H. V. Winsor, USAF
Bolling AFB
Washington, DC 20332

Department of Commerce
National Bureau of Standards
Attn Library
Washington, DC 20234

NASA Langley Research Center
Attn N. P. Barnes (2 copies)
Attn G. Armagan

NASA Langley Research Center (cont'd)
Attn P. Cross
Attn D. Getteny
Attn J. Barnes
Attn E. Filer
Attn C. Bair
Attn N. Bounchrishani
Hampton, VA 23665

Director
Advisory Group on Electron Devices
Attn Sectry, Working Group D
201 Varick Street
New York, NY 10013

Aerospace Corporation
Attn M. Birnbaum
Attn N. C. Chang
PO Box 92957
Los Angeles, CA 90009

Allied Signal Inc
Advanced Application Dept
Attn A. Budgor
31717 La Tiemda Drive
Westlake Village, CA 91362

Allied Signal Inc
Attn Y. Band
Attn R. Morris
POB 1021R
Morristown, NJ 07960

Ames Laboratory Dow
Iowa State University
Attn K. A. Gschneidner, Jr (2 copies)
Ames, IA 50011

Argonne National Laboratory
Attn W. T. Carnall
9700 South Cass Avenue
Argonne, IL 60439

Booz, Allen and Hamilton
Attn W. Drozdoski
4330 East West Highway
Bethesda, MD 20814

Distribution (cont'd)

Brimrose Corp of America
Attn R. G. Rosemeier
7527 Belair Road
Baltimore, MD 21236

Draper Lab
Attn F. Hakimi, MS 53555 Tech Sq
Cambridge, MA 02139

Engineering Societies Library
Attn Acquisitions Dept
345 East 47th Street
New York, NY 10017

Fibertech Inc
Attn H. R. Verdun (3 copies)
510-A Herdon Pkwy
Herdon, VA 22070

General Dynamics
Attn R. J. Blair
5452 Oberlin Drive
San Diego, CA 92121

Hughes Aircraft Company
Attn D. Sumida
3011 Malibu Canyon Rd
Malibu, CA 90265

IBM Research Division
Almaden Research Center
Attn R. M. Macfarlane, Mail Stop K32 802(d)
650 Harry Road
San Jose, CA 95120

Director
Lawrence Radiation Laboratory
Attn M. J. Weber
Attn H. A. Koehler
Attn W. Krupke
Livermore, CA 94550

LTV
Attn M. Kock (WT-50)
PO Box 650003
Dallas, TX 75265

Martin Marietta
Attn F. Crowne
Attn J. Little, 1450

Martin Marietta (cont'd)
Attn T. Worchesky
1450 South Rolling Road
Baltimore, MD 21227

McDonnell Douglass Electronic Systems Company
Dept Y440, Bldg. 101, Lev. 2 Rm/Pt B54
Attn D. M. Andrauskas, MS-2066267
PO Box 516
St Louis, MO 63166

MIT Lincoln Lab
Attn B. Aull
PO Box 73
Lexington, MA 02173

Department of Mechanical, Industrial, & Aerospace Engineering
Attn S. Temkin
PO Box 909
Piscataway, NJ 08854

National Oceanic & Atmospheric Adm Environmental Research Labs
Attn Library, R-51, Tech Rpts
Boulder, CA 80302

Oak Ridge National Laboratory
Attn R. G. Haire
Oak Ridge, TN 37839

W. J. Schafer Assoc
Attn J. W. Collins
321 Billerica Road
Chelmsford, MA 01824

Science Applications, International Corp
Attn T. Allik
1710 Goodridge Drive
McLean, VA 22102

Shwartz Electro-Optic, Inc.
Attn G. A. Rines
45 Winthrop Street
Concord, MA 01742

Distribution (cont'd)

Teledyne Brown Engineering
Cummings Research Park
Attn M. L. Price, MS-44
Huntsville, AL 35807

Union Carbide Corp
Attn M. R. Kokta
50 South 32nd Street
Washougal, WA 98671

Arizona State University
Dept of Chemistry
Attn L Eyring
Tempe, AZ 85281

University of Southern California
Attn Dr. M. Birnbaum
Denney Research Bldg., University Park
Los Angeles, CA 90089

Carnegie Mellon University
Schenley Park
Attn Physics & EE, J. O. Artman
Pittsburgh, PA 15213

Colorado State University
Physics Department
Attn S. Kern
Ft Collins, CO 80523

University of Connecticut
Department of Physics
Attn R. H. Bartram
Attn R. Sinkovits
Storrs, CT 06269

University of South Florida
Physics Dept
Attn R. Chang
Attn Sengupta
Tampa, FL 33620

Howard University
Physics Department
Attn Prof. V. Kushamaha
25 Bryant St., N.W.
Washington, DC 20059

Johns Hopkins University
Dept of Physics
Attn B. R. Judd
Baltimore, MD 21218

Kalamazoo College
Dept of Physics
Attn K. Rajnak
Kalamazoo, MI 49007

Massachusetts Institute of Technology
Crystal Physics Laboratory
Attn H. P. Jenssen
Attn A. Linz
Cambridge, MA 02139

Massachusetts Institute of Technology
Attn V. Bagnato
77 Mass Ave, Room 26-251
Cambridge, MA 02139

University of Michigan
Dept of Physics
Attn S. C. Rand
Ann Arbor, MI 48109

University of Minnesota, Duluth
Department of Chemistry
Attn L. C. Thompson
Duluth, MN 55812

Oklahoma State University
Dept of Physics
Attn R. C. Powell
Stillwater, OK 74078

Pennsylvania State University
Materials Research Laboratory
Attn W. B. White
University Park, PA 16802

Princeton University
Department of Chemistry
Attn D. S. McClure
Attn C. Weaver
Princeton, NJ 08544

Distribution (cont'd)

San Jose State University
Department of Physics
Attn J. B. Gruber
San Jose, CA 95192

Seaton Hall University
Chemistry Department
Attn H. Brittain
South Orange, NJ 07099

University of Virginia
Dept of Chemistry
Attn F. S. Richardson (2 copies)
Charlottesville, VA 22901

University of Wisconsin
Chemistry Department
Attn J. Wright
Attn B. Tissue
Madison, WI 53706

US Army Laboratory Command
Attn Technical Director, AMSLC-TD

Installation Support Activity
Attn Legal Office, SICIS-CC

USAISC
Attn Administrative Services Branch, AMSLC-IM-TS
Attn Technical Publishing Branch, AMSLC-IM-VP (2 copies)

Harry Diamond Laboratories
Attn Division Directors
Attn Library, SLCHD-TL (3 copies)
Attn Library, SLCHD-TL (Woodbridge)
Attn Chief, SLCHD-NW-CS
Attn Chief, SLCHD-NW-E
Attn Chief, SLCHD-NW-EH
Attn Chief, SLCHD-NW-EP
Attn Chief, SLCHD-NW-ES
Attn Chief, SLCHD-NW-P
Attn Chief, SLCHD-NW-R
Attn Chief, SLCHD-NW-RP

Harry Diamond Laboratories (cont'd)
Attn Chief, SLCHD-NW-RS
Attn Chief, SLCHD-NW-TN
Attn Chief, SLCHD-NW-TS
Attn Chief, SLCHD-PO
Attn Chief, SLCHD-ST-C
Attn Chief, SLCHD-ST-RP
Attn Chief, SLCHD-ST-RS
Attn Chief, SLCHD-TT
Attn B. Willis, SLCHD-TA-ET
Attn B. Zabludowski, SLCHD-TA-ET
Attn C. S. Kenyon, SLHD-NW-EP
Attn J. R. Miletta, SLCHD-NW-EP
Attn F. B. McLean, SLCHD-ST-MW
Attn L. Libelo, SLCHD-ST-MW
Attn A. A. Bencivenga, SLCHD-ST-SP
Attn J. Sattler, SLCHD-CS
Attn J. Nemarich, SLCHD-ST-CB
Attn B. Weber, SLCHD-ST-CB
Attn T. Bahder, SLCHD-ST-AP
Attn J. Bradshaw, SLCHD-ST-AP
Attn J. Bruno, SLCHD-ST-AP
Attn E. Harris, SLCHD-ST-AP
Attn R. Leavitt, SLCHD-ST-AP
Attn J. Pham, SLCHD-ST-AP
Attn G. Simonis, SLCHD-ST-AP
Attn M. Stead, SLCHD-ST-AP
Attn J. Stellato, SLCHD-ST-AP
Attn S. Stevens, SLCHD-ST-AP
Attn R. Tober, SLCHD-ST-AP
Attn M. Tobin, SLCHD-ST-AP
Attn G. Turner, SLCHD-ST-AP (10 copies)
Attn D. Wortman, SLCHD-ST-AP
Attn C. Garvin, SLCHD-ST-SS
Attn J. Goff, SLCHD-RT-RB
Attn C. Morrison, SLCHD-ST-AP (10 copies)